Hydrolysis of Monobutyltin Trialkoxides: Synthesis and Characterizations of $\{(BuSn)_{12}O_{14}(OH)_6\}(OH)_2$

Frédéric Banse, F. Ribot,* P. Tolédano, J. Maquet, and C. Sanchez

Chimie de la Matière Condensée (URA 1466), Université Pierre et Marie Curie, 75252 Paris, France

Received February 9, 1995[⊗]

Hydrolysis-condensation of butyltin triisopropoxide and butyltin tri-*tert*-amyloxide with more than three water molecules per tin atom yields only the cagelike oxo−hydroxo butyltin cluster, $\{(BuSn)_{12}O_{14}(OH)_6\}(OH)_2$. Its molecular structure has been resolved by X-ray diffraction in the crystalline compound $\{(BuSn)_{12}(\mu_3\text{-}O)_{14}(\mu_2\text{-}OH)_6\}(OH)_2(HOPr^i)_4$. This cluster has also been characterized in solution by ^{119}Sn, ^1H, and ^{13}C NMR spectroscopies. The $^{119}Sn-^{119/117}Sn$ two bond coupling satellites oberved in the solution ^{119}Sn NMR spectrum have allowed measurement of four scalar coupling constants that can be correlated to the Sn−O−Sn framework. Two dimensional NMR experiments have unambiguously allowed assignment of all the ^1H and ^{13}C resonances of the cluster and showed that the coordination of tin is felt, at least, up to the third carbon of the butyl chains. The ^{119}Sn MAS NMR technique was also used to characterize solid compounds. The shielding tensorial properties are reported and discussed in relation to the oxo−hydroxo butyltin cluster structure.

Introduction

Monoalkyltin compounds exhibit a rich oxo-clusters chemistry with many different structures.[1] Most of them have been prepared by reaction of organostannonic acids with carboxylic or phosphinic acids or by reaction of monoorganotin trichlorides with silver carboxylates.[1] In those cases, carboxylates (i.e., $[PhSn(O)O_2CC_6H_{11}])_6$)[2] or phosphinates (i.e., $[(n\text{-}BuSn(OH)O_2PPh_2)_3O][O_2PPh_2]$)[3] are found in the final compounds, usually allowing a coordination number of 6 for tin. Other monoalkyltin oxo clusters have also been prepared by the base hydrolysis of monoalkyltin trichlorides.[4−9] With such a method, chloride is always present in the final compounds (i.e., $\{(BuSn)_{12}O_{14}(OH)_6\}Cl_2\cdot 2H_2O$).[9]

Hydrolysis of metal alkoxides provide another way to synthesize oxo−hydroxo species under mild chemical conditions (organic solvents, room temperature).[10−12] Moreover, this method avoids the presence of chloride in the final compounds. This synthesis route, maybe because of the commercial unavailability of the corresponding precursors, was almost never evaluated for the preparation of monoorganotin oxo clusters.[13,14]

Our interest in the organotin oxo species, especially the closo-type ones, is their potential use as well-defined inorganic entities for the elaboration of hybrid organic−inorganic materials.[11,14−22] A special type of materials can be elaborated from such well-defined performed clusters, which are then embedded in organic polymers or assembled, through covalent bonds, by organic chains. These materials, in which the size of the inorganic part is perfectly controlled, are interesting models for understanding organic−inorganic nanocomposites of less-defined nanostructure. Materials, based on the attachment of nano-building blocks, have for the moment only been prepared from organosilicon oxo species[20,21] and organosilicon modified polyoxotungstates.[22] This paper deals with the preparation, by hydrolysis of butyltin trialkoxides, of the oxo−hydroxo butyltin cluster $\{(BuSn)_{12}O_{14}(OH)_6\}(OH)_2$. Its molecular structure is determined, by X-ray diffraction, on crystalline $\{(BuSn)_{12}O_{14}(OH)_6\}(OH)_2(HOPr^i)_4$. NMR characterizations of the oxo−hydroxo butyltin cluster, including ^{119}Sn (solution and solid state), ^1H, ^{13}C, and correlation spectroscopies, are also reported.

Experimental Section

Precursors Synthesis. *n*-Butyltin trialkoxides were synthesized by reacting stoichiometric amounts of sodium alkoxide with *n*-butyltin trichloride.[23] 1,2-Dimethoxyethane (DME) was used as cosolvent, instead of benzene, to ease the filtration separation step. All the experiments were carried out with Schlenk-line techniques to avoid hydrolysis of the compounds.[24] Sodium isopropoxide was prepared from metallic sodium and sodium *tert*-amyloxide from sodium hydride. To a boiling solution of the desired sodium alkoxide (0.426 mol in

[⊗] Abstract published in *Advance ACS Abstracts,* November 1, 1995.

(1) Holmes, R. R. *Acc. Chem. Res.* **1989**, *22*, 190.
(2) Chandrasekhar, V.; Day, R. O.; Holmes, R. R. *Inorg. Chem.* **1985**, *24*, 1970.
(3) Day, R. O.; Holmes, J. M.; Chandrasekhar, V.; Holmes, R. R. *J. Am. Chem. Soc.* **1987**, *109*, 940.
(4) Lecomte, C.; Protas, J.; Devaud, M. *Acta Crystallogr.* **1975**, *B32*, 923.
(5) Puff, H.; Reuter, H. *J. Organomet. Chem.* **1989**, *364*, 57.
(6) Puff, H.; Reuter, H. *J. Organomet. Chem.* **1989**, *368*, 173.
(7) Puff, H.; Reuter, H. *J. Organomet. Chem.* **1989**, *373*, 173.
(8) Reuter, H. *Angew. Chem.* **1991**, *103*, 1487.
(9) Dakternieks, D.; Zhu, H.; Tiekink, E. R. T.; Colton, R. *J. Organomet. Chem.* **1994**, *476*, 33.
(10) Sanchez, C.; Ribot, F.; Doeuff, S. In *Inorganic and Organometallic Polymers with Special Properties*; Laine, R. M., Ed.; NATO ASI Series Vol. 206, Kluwer Academic Publisher: Dordrecht, The Netherlands, 1992; p 267.
(11) Sanchez, C.; Ribot, F. *New J. Chem.* **1994**, *18*, 1007.
(12) Day, V. W.; Eberspacher, T. A.; Chen, Y.; Hao, J.; Klemperer, W. G. *Inorg. Chem. Acta* **1995**, *229*, 391.
(13) Ribot, F.; Banse, F.; Sanchez, C. *Mater. Res. Soc. Symp. Proc.* **1992**, *271*, 45.
(14) Ribot, F.; Banse, F.; Sanchez, C. *Mater. Res. Soc. Symp. Proc.* **1994**, *346*, 121.
(15) Schmidt, H.; Scholze, H.; Kaiser, A. *J. Non-Cryst. Solids* **1984**, *63*, 1.
(16) Wilkes, G. L.; Orler, B.; Huang, H. H. *Polym. Prepr.* **1985**, *26*, 300.
(17) Sur, G.-S.; Mark, J. E. *Eur. Polym. J.* **1985**, *21*, 1051.
(18) Boulton, J. M.; Thompson, J.; Fox, H. H.; Gorodisher, I.; Teowee, G.; Calvert, P. D.; Ulhmann, D. R. *Mater. Res. Soc. Symp. Proc.* **1990**, *180*, 987.
(19) Novak, B. M. *Adv. Mater.* **1993**, *6*, 422.
(20) Hoebbel, D.; Pitsch, I.; Heidemann, D.; Jancke, H.; Hiller, W. *Z. Anorg. Allg. Chem.* **1990**, *583*, 133.
(21) Hoebbel, D.; Pitsch, I.; Heidemann, D. *Z. Anorg. Allg. Chem.* **1991**, *592*, 207.
(22) Judenstein, P. *Chem. Mater.* **1991**, *4*, 4.
(23) Gaur, D. P.; Srivastava, G.; Mehrotra, R. C. *J. Organomet. Chem.* **1973**, *63*, 221.
(24) Shriver, D. F. *The Manipulation of Air Sensitive Compounds*; McGraw-Hill Book Co.: New York, 1969.

0020-1669/95/1334-6371$09.00/0

100 mL of DME and 50 mL of $HOPr^i$ or 100 mL of DME and 50 mL of $HOAm^t$) $BuSnCl_3$ (0.142 mol in 100 mL of DME) was added drop by drop. These mixtures were refluxed for 3 h and then allowed to cool. Sodium chloride, formed during the reaction, was removed by filtration. Excess solvents were evaporated under reduced pressure. Finally, *n*-butyltin trialkoxides were distilled under vacuum.

$BuSn(OPr^i)_3$: bp = 70 °C/0.004 mmHg; white solid (T_f = 38 °C); yield = 70%; $\delta(^{119}Sn)$ = −321 ppm vs $Sn(CH_3)_4$ (2.5 M in C_6D_6).

$BuSn(OAm^t)_3$: bp = 62 °C/0.002 mmHg; clear liquid; yield = 70%; $\delta(^{119}Sn)$ = −194 ppm vs $Sn(CH_3)_4$ in C_6D_6.

Hydrolysis Experiments. Water (460 μL) was slowly added to a stirred solution of $BuSn(OPr^i)_3$ (3 g, 8.5 × 10^{-3} mol, H_2O/Sn = 3) in isopropyl alcohol (0.5 g, 8.5 × 10^{-3} mol), resulting in a turbid mixture from which rectangular shaped X-ray quality crystals grew, reproducibly, within a few weeks at room temperature. In the following these crystals are referred to as compound **C1**. These crystals are colorless in their mother liquor but turn white upon standing in air. Moreover, they undergo amorphization and become insoluble in C_6D_6 or CD_2Cl_2 as their aspect changes. Therefore, crystals of **C1** were, just after removal from their mother liquor, either dissolved in deuterated solvent for solution NMR studies or conditioned in a tight closed rotor for solid state NMR. Chemical analysis performed on **C1**, dried one night in air, lead to the following. Anal. Found for $\{(BuSn)_{12}O_{14}(OH)_6\}(OH)_2$: Sn, 56.8%; C, 23.4%; H, 4.9%; O, 14.9%. Calcd: Sn, 57.7%, C, 23.3%; H, 4.7%; O, 14.3%.

To stirred liquid $BuSn(OPr^i)_3$ (9.9 g, 2.8 × 10^{-2} mol, $T \approx 45$ °C) was added, drop by drop, a mixture of 5.04 g of water (H_2O/Sn = 10) and 45.36 g of isopropyl alcohol. The final clear solution (**S2**), kept at −5 °C, yielded, in a reproducible way, a fine precipitate over night. A 3 g amount of solid was isolated by filtration. This solid (**P2**) also becomes insoluble when standing in air for a few hours. Therefore, it was, just after filtration, either dissolved in deuterated solvent for solution NMR studies or conditioned in a tight closed rotor for solid state NMR. Chemical analysis performed on **P2**, dried one night in air, lead to the following. Anal. Found for $\{(BuSn)_{12}O_{14}(OH)_6\}(OH)_2$: Sn, 56.8%; C, 23.8%; H, 4.8%; O, 14.2%. Calcd: Sn, 57.7%; C, 23.3%; H, 4.7%, O, 14.3%. A total amount of 4 g of **P2** can be obtained by successive crystallizations of the mother liquor (yield = 67% relative to $\{(BuSn)_{12}O_{14}(OH)_6\}(OH)_2$). The precipitate **P2** was also prepared following the same procedure, but with other H_2O/Sn ratios (ranging from 4 to 10). No change was observed in the total crystallization yield with different hydrolysis ratios.

To stirred $BuSn(OAm^t)_3$ (4.8 g, 1.1 × 10^{-2} mol; room temperature) was added drop by drop to a mixture of 1.98 g of water (H_2O/Sn = 10) and 17.82 g of *tert*-amyl alcohol. The final clear solution (**S3**), kept at −5 °C, gave no precipitate in several days.

Crystal Structure Determination. Crystals **C1** were of sufficient quality to perform a single X-ray diffraction study. To avoid amorphization, the analyzed crystals were conditioned in a Lindman sealed capillary just after being removed from their mother liquor. Determination of lattice constants and collection of intensity data were performed at 293 K on an Enraf-Nonius CAD4 diffractometer using Mo Kα radiation and graphite monochromator. Unit cell parameters were derived from a least squares refinement of the setting angles of 25 randomly selected reflections in the range 14.6° ≤ θ ≤ 15.0°. Intensity data were collected using a variable speed ω/2θ-scan mode ($\Delta\omega = 0.80 + 0.34tg(\theta)$°; variable ω scan speed from 1.8 to 20.1 deg/min depending on the diffracted intensity) and corrected for Lorentz and polarization effects. The intensities and orientation of two standard reflections were monitored every hour and 100 reflections, and showed no significant variation (lower than 1%).

The space group *C2/c* was established from systematic extinctions. Tin atoms were localized by direct methods using SHELXS86.[25] The structure was then resolved by difference Fourier syntheses and full-matrix least squares refinements, using CRYSTALS[26] on a Dell 333D microcomputer (80386 processor at 33 MHz). An absorption correction was performed using DIFABS.[27] After the anisotropic refinement of all the non-hydrogen atoms, the positions of the hydrogen atoms were calculated. Two isotropic thermal parameters, one for the hydrogen atoms bound to an oxygen atom and another for hydrogen atoms bound to a carbon atom, were refined. Finally, 446 parameters were considered during refinement: scale factor, secondary extinction coefficient,[28] atomic coordinates, and thermal parameters (anisotropic except for hydrogen atoms). Crystal data, data collection parameters, and residual from refinement are summarized in Table 1. The ORTEP[29] drawing of **C1** is presented in Figure 1.

Table 1. Crystallographic Data for **C1**

Crystal Data	
$Sn_{12}C_{60}H_{148}O_{26}$	ϱ_{calcd} = 1.84 g cm^{-3}
fw = 2710.1	λ = 0.710 69 Å (Mo Kα)
monoclinic: *C2/c* (No. 15)	cell parameters from 25 reflections
a = 33.445(8) Å	θ = 14.6−15°
b = 12.797(5) Å	μ = 3.08 mm^{-1}
c = 27.090(9) Å	temp = 293 K
β = 122.39(2)°	parallelepiped: 0.5 × 0.3 × 0.3 mm
V = 9790(116) Å^3	*F*(000) = 5264
Z = 4	colorless
Data Collection	
Enraf-Nonius CAD-4 diffractometer	θ max = 23°
ω/2θ scans	*h* = −36 → 30
adsorpn correcns: empirical (DIFABS)	*k* = 0 → 14
T_{min} = 0.673, T_{max} = 1.587	*l* = 0 → 29
no. of data collecd = 7479	
no of unique data = 6788	2 std reflecns monitored every 100 reflecns and 60 min
no. of data with $I > 3\sigma(I)$ = 3863	
R_{int} = 0.0525	intensity variation: 1%
Refinement[a]	
refinement on *F*	$(\Delta/\sigma)_{max}$ = 0.017
R = 0.0339	$\Delta\rho_{max}$ = 0.43 e Å^{-3}
R_w = 0.0342 with *w* = 1	$\Delta\rho_{min}$ = −0.39 e Å^{-3}
S = 1.92	extincn correcn: Larson[28]
3863 reflecns	secondary extincn coeff: 17.5(6)
446 params refined	atomic scattering factors: *International Tables for X-Ray Crystallography*
only H atoms *U*'s refined	

[a] $R = \sum(||F_o| - |F_c||)/\sum|F_o|$; $R_w = [\sum(w|F_o - F_c|^2)/\sum(wF_o^2)]^{1/2}$; $S = [\sum w(|F_o| - |F_c|)^2/(m - n)]^{1/2}$.

NMR Spectroscopy. ^{119}Sn solution NMR experiments (1D and 2D $^{119}Sn-^1H$) were performed on a Bruker AM250 spectrometer (250.13 MHz for ^1H and 93.27 MHz for ^{119}Sn). Proton decoupled spectra were obtained with a composite pulse decoupling sequence (CPD). ^{119}Sn chemical shifts are relative to external tetramethyltin (TMT). Deuterated solvents (CD_2Cl_2 or C_6D_6) were used as internal lock. For the $^{119}Sn-^1H$ heteronuclear shift correlated 2D NMR,[30] 128 increments were performed, and the delay ($^1/_2J$) was set to 4.5 ms, which corresponds to a J_{Sn-H} value of about 110 Hz.

^1H and ^{13}C solution NMR experiments were performed on a Bruker AC300 spectrometer (300.13 MHz for ^1H and 75.47 MHz for ^{13}C). CD_2Cl_2 was used as solvent and internal lock. Chemical shifts are relative to TMS, using the solvent or its protonated impurities as secondary internal reference ($\delta(^1H)$ = 5.33 ppm vs TMS and $\delta(^{13}C)$ = 53.6 ppm vs TMS). $^1H-^1H$ COSY NMR[31] was performed with a 90° mixing pulse. For ^{13}C refocused and decoupled INEPT, mixing (2 ms) and refocusing times (3 ms, CH_3 and CH positive, CH_2 negative) were

(25) Sheldrick, G. M. *SHELXS86*, Program for the solution of crystal structures; University of Göttingen: Göttingen, 1986.
(26) Watkin, D. J.; Carruthers, J. R.; Betteridge, P. W. *CRYSTALS*, An advanced crystallographic program system; Chemical Crystallography Laboratory, University of Oxford: Oxford, U.K., 1988.
(27) Walker, N.; Stuart, D. *Acta Crystallogr.* **1983**, *A39*, 158.
(28) Larson, C. K. In *Crystallographic Computing*; Ahmed, F. R., Hall, S. R., Huber, C. P., Eds.; Munkgaard: Copenhagen, Denmark, 1970; p 291.
(29) Johnson, C. K. *ORTEPII*; ORNL-5138 report, Oak Ridge National Laboratory: Oak Ridge, TN, 1976.
(30) Bax, A.; Morris, G. *J. Magn. Reson.* **1981**, *42*, 501.
(31) Aue, W. P.; Bartholdi, E.; Ernst, R. R. *J. Chem. Phys.* **1976**, *64*, 2226.

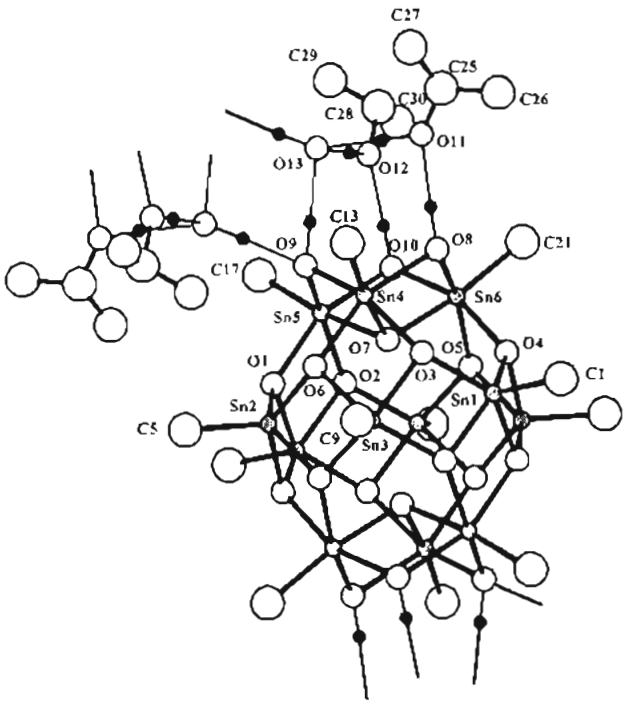

Figure 1. ORTEP[29] drawing of **C1** with arbitrary diameter for all atoms. Hydrogen atoms involved in the hydrogen bonding framework are represented as small black spheres. Hydrogen bonds are visualized as fine lines. Only the first carbon atom of every butyl chain has been represented for clarity.

set in agreement with a J^1_{C-H} value of 125 Hz. For 2D $^{13}C-^1H$ heteronuclear shift correlated 2D NMR[30] (128 increments in ^1H dimension), a delay of 4 ms corresponding also to $J^1_{C-H} = 125$ Hz was chosen.

^{119}Sn MAS NMR experiments were performed on a Bruker MSL300 spectrometer (111.89 MHz for ^{119}Sn) equipped with a 4 mm locked Bruker probe (pulse angle $\approx 30°$, recycle delay = 10 s). Chemical shifts are relative to TMT, using the ^{119}Sn resonance of solid tetracyclohexyltin ($\delta = -97.35$ ppm) as secondary external reference.[32] At least two experiments, with sufficiently different rotation speeds, were run to locate isotropic chemical shifts. ^{119}Sn shielding tensorial values were analyzed with WINFIT software[33] using the Herzfeld and Berger approach.[34] They are reported, following Haeberlen's notation,[35] as the isotropic chemical shift ($\delta_{iso} = -\sigma_{iso}$), the anisotropy ($\delta_A = \sigma_{33} - \sigma_{iso}$), and the asymmetry ($\eta = |\sigma_{22} - \sigma_{11}|/|\sigma_{33} - \sigma_{iso}|$), with $|\sigma_{33} - \sigma_{iso}| \geq |\sigma_{11} - \sigma_{iso}| \geq |\sigma_{22} - \sigma_{iso}|$.

Results

Molecular Structure of $\{(BuSn)_{12}(\mu_3\text{-}O)_{14}(\mu_2\text{-}OH)_6\}(OH)_2(HOPr^i)_4$ (C1). The ORTEP[29] drawing of **C1** is presented in Figure 1. The structure is based on a centrosymmetric macrocation $\{(BuSn)_{12}O_{14}(OH)_6\}^{2+}$ which is composed of twelve tin atoms (six unequivalent) linked by μ_3-O and μ_2-OH bridges. The Sn−O−Sn framework forms an almost spherical cage, and a butyl chain is attached to every tin atom. Six tin atoms (Sn(1), Sn(2), Sn(3), and their symmetrics) are five-coordinate (labeled Sn_p) and exhibit distorted square pyramidal environment. The other six (Sn(4), Sn(5), Sn(6), and their symmetrics) are six-coordinate (Sn_o) and exhibit distorted octahedral geometry. The μ_2-OH bridges (O(8), O(9), O(10), and their symmetrics) are only involved in the coordination of six-coordinate tin atoms. One μ_3-O bridge (O(7)) links the three unequivalent six-coordinate tin atoms. All the other μ_3-O bridges (O(1), O(2), O(3), O(4), O(5), O(6), and their symmetrics) connect five- and six-coordinate tin atoms together. This oxo−hydroxo butyltin core can be mentally split in three subunits. Two are trimeric "$(BuSn)_3(\mu_3\text{-}O)(\mu_2\text{-}OH)_3$" and contain six-coordinate tin atoms only. The other one is a hexameric cycle "$(BuSn)_6(\mu_2\text{-}O)_{12}$", where tin atoms are only five coordinate. The cage is obtained by capping each side of the hexameric cycle by a trimeric unit.

The positive charge of the macro-cation is compensated by two hydroxyl groups (O(13) and its symmetric). Each hydroxyl counter-ion exchanges hydrogen bonds with two μ_2-OH bridges (O(9) and its symmetric) belonging to two different clusters. These hydrogen bonds leads to the formation of cluster chains, parallel to the *b* axis of the structure. Four isopropyl alcohol molecules (corresponding to the oxygen atoms O(11), O(12), and their symmetrics) are also found in the structure. Each of them are linked through hydrogen bonds to a μ_2-OH bridge of the macro-cation and to a hydroxyl counterion (O(11) to O(8) and O(13); O(12) to O(10) and O(13)). Note that the μ_2-OH

Table 2. Fractional Atomic Coordinates with Esd's in Parentheses and Equivalent Isotropic Thermal Parameters[a] (Å^2) for **C1**

atom	*x/a*	*y/b*	*z/c*	U_{eq}
Sn(1)	0.10515(3)	0.03945(7)	0.10409(4)	0.0663
Sn(2)	−0.01965(3)	−0.11953(7)	−0.11467(4)	0.0694
Sn(3)	0.08355(3)	−0.03639(7)	−0.01944(4)	0.0664
Sn(4)	0.05796(3)	−0.23472(7)	0.03813(4)	0.0674
Sn(5)	−0.05221(3)	−0.23624(6)	−0.01086(4)	0.0671
Sn(6)	0.02124(3)	−0.13735(7)	0.12003(4)	0.0688
O(1)	−0.0638(3)	−0.1710(6)	−0.0908(3)	0.0701
O(2)	−0.0932(3)	−0.0967(5)	−0.0257(3)	0.0644
O(3)	0.1003(2)	−0.0937(6)	0.0612(3)	0.0638
O(4)	0.0661(3)	−0.0065(6)	0.1370(3)	0.0712
O(5)	−0.0249(2)	−0.0080(6)	0.0965(3)	0.0687
O(6)	0.0415(3)	−0.1711(6)	−0.0430(3)	0.0698
O(7)	0.0067(2)	−0.1361(5)	0.0360(3)	0.0612
O(8)	0.0739(3)	−0.2368(6)	0.1265(3)	0.0787
O(9)	0.0004(3)	−0.3319(5)	0.0003(4)	0.0709
O(10)	−0.0373(3)	−0.2384(6)	0.0763(3)	0.0777
O(11)	0.0926(5)	−0.4339(9)	0.1720(5)	0.1391
O(12)	−0.0368(5)	−0.4362(9)	0.1132(6)	0.1313
O(13)	0.0149(3)	−0.5048(6)	0.0697(4)	0.0862
C(1)	0.1751(5)	0.074(1)	0.1730(7)	0.1011
C(2)	0.2051(7)	−0.012(3)	0.210(1)	0.1944
C(3)	0.1931(7)	−0.092(3)	0.226(1)	0.1729
C(4)	0.2285(9)	−0.167(3)	0.266(1)	0.2555
C(5)	−0.0335(6)	−0.191(1)	−0.1932(7)	0.1118
C(6)	−0.0855(8)	−0.169(2)	−0.2449(8)	0.1437
C(7)	−0.094(1)	−0.212(3)	−0.300(1)	0.2051
C(8)	−0.144(1)	−0.195(3)	−0.342(1)	0.2494
C(9)	0.1413(5)	−0.059(1)	−0.0307(7)	0.0911
C(10)	0.1896(5)	−0.036(2)	0.0245(8)	0.1117
C(11)	0.2281(7)	−0.057(2)	0.014(1)	0.1872
C(12)	0.2735(9)	−0.032(4)	0.067(1)	0.2895
C(13)	0.1118(6)	−0.341(1)	0.0503(7)	0.0977
C(14)	0.1617(6)	−0.305(1)	0.091(1)	0.1464
C(15)	0.1968(8)	−0.383(2)	0.092(2)	0.1837
C(16)	0.239(1)	−0.348(3)	0.124(3)	0.3961
C(17)	−0.1077(6)	−0.348(1)	−0.0484(8)	0.1072
C(18)	−0.156(1)	−0.320(2)	−0.064(1)	0.2088
C(19)	−0.162(1)	−0.295(2)	−0.021(1)	0.1948
C(20)	−0.2166(9)	−0.296(3)	−0.044(1)	0.2403
C(21)	0.0359(5)	−0.159(1)	0.2071(6)	0.0903
C(22)	0.0880(6)	−0.159(1)	0.2551(6)	0.1080
C(23)	0.0951(8)	−0.164(2)	0.3163(8)	0.1404
C(24)	0.1461(9)	−0.167(2)	0.3610(9)	0.1995
C(25)	0.125(1)	−0.490(2)	0.214(1)	0.1825
C(26)	0.162(1)	−0.432(2)	0.263(1)	0.2295
C(27)	0.136(1)	−0.586(2)	0.207(1)	0.2242
C(28)	−0.045(1)	−0.500(2)	0.146(1)	0.1875
C(29)	−0.068(1)	−0.587(3)	0.116(1)	0.2726
C(30)	−0.079(2)	−0.453(2)	0.155(2)	0.2789

[a] $U_{eq} = {}^1/_3\sum_i\sum_j U_{ij}a_i^*a_j^*\mathbf{a}_i\mathbf{a}_j$

(32) Reuter, H.; Sebald, A. *Z. Naturforsch.* **1992**, *48b*, 195.
(33) Massiot, D.; Thiele, H.; Germanus, A. *Bruker Rep.* **1994**, *140*, 43.
(34) Herzfeld, J.; Berger, A. E. *J. Chem. Phys.* **1980**, *73*, 6021.
(35) Haeberlen, U. *Adv. Magn. Reson. Suppl. 1* **1976**.

Table 3. Selected Interatomic Distances (Å) and Bond Angles (deg) with Esd's in Parentheses for **C1** (Symmetry Code: (i) $-x, -y, -z$)

$\langle Sn_p-O\rangle^a$	2.084	$\langle Sn_p-O\rangle$	2.023	$\langle Sn_o-O\rangle$	2.140	$\langle Sn_p\text{-}Sn_p\rangle$	3.184	$\langle Sn_p\text{-}Sn_o\rangle$	3.827	$\langle Sn_o\text{-}Sn_o\rangle$	3.259
Sn(1)−O(1)^i	2.084(8)	Sn(1)−O(3)	2.019(7)	Sn(4)−O(3)	2.169(7)	Sn(1)−Sn(2)^i	3.192(1)	Sn(1)−Sn(4)	3.869(1)	Sn(4)−Sn(5)	3.178(1)
Sn(1)−O(2)^i	2.074(7)	Sn(1)−O(4)	2.021(7)	Sn(4)−O(6)	2.122(8)	Sn(1)−Sn(3)	3.174(1)	Sn(1)−Sn(6)	3.805(1)	Sn(4)−Sn(6)	3.302(1)
Sn(2)−O(4)^i	2.092(8)	Sn(2)−O(1)	2.014(8)	Sn(5)−O(1)	2.153(8)	Sn(2)−Sn(3)	3.187(1)	Sn(2)−Sn(4)	3.812(1)	Sn(5)−Sn(6)	3.298(1)
Sn(2)−O(5)^i	2.083(7)	Sn(2)−O(6)	2.032(8)	Sn(5)−O(2)	2.154(7)	$\langle Sn_p\text{-}Sn_o\rangle$	3.313	Sn(2)−Sn(5)	3.822(1)	$\langle O-H-O\rangle$	2.74
Sn(3)−O(3)	2.076(7)	Sn(3)−O(2)^i	2.019(7)	Sn(6)−O(4)	2.129(8)	Sn(1)−Sn(5)^i	3.326(1)	Sn(3)−Sn(5)^i	3.856(1)	O(8)−O(11)	2.73(1)
Sn(3)−O(6)	2.097(7)	Sn(3)−O(5)^i	2.035(7)	Sn(6)−O(5)	2.115(8)	Sn(2)−Sn(6)^i	3.290(1)	Sn(3)−Sn(6)^i	3.797(1)	O(9)−O(13)	2.77(1)
$\langle Sn_o-O\rangle$	2.091	$\langle Sn_o-OH\rangle$	2.096	$\langle Sn_o-C\rangle$	2.14	Sn(3)−Sn(4)	3.322(1)			O(10)−O(12)	2.72(1)
Sn(4)−O(7)	2.106(7)	Sn(4)−O(8)	2.157(8)	Sn(4)−C(13)	2.14(1)					O(11)−O(13)	2.75(1)
Sn(5)−O(7)	2.110(7)	Sn(4)−O(9)	2.047(8)	Sn(5)−C(17)	2.12(2)					O(12)−O(13)	2.71(1)
Sn(6)−O(7)	2.057(7)	Sn(5)−O(9)	2.027(8)	Sn(6)−C(21)	2.16(1)						
		Sn(5)−O(10)	2.136(8)	$\langle Sn_p-C\rangle$	2.123						
		Sn(6)−O(8)	2.103(8)	Sn(1)−C(1)	2.11(1)						
		Sn(6)−O(10)	2.103(8)	Sn(2)−C(5)	2.13(1)						
				Sn(3)−C(9)	2.13(1)						
$\langle O-Sn_p-O\rangle_c{}^b$	78.0	$\langle O-Sn_p-O\rangle_c$	97.6	O(4)−Sn(1)−C(1)	109.9(5)	O(10)−Sn(5)−C(17)	98.5(6)				
O(1)^i−Sn(1)−O(2)^i	78.0(3)	O(3)−Sn(1)−O(4)	97.8(3)	O(1)−Sn(2)−C(5)	112.1(5)	O(8)−Sn(6)−C(21)	98.0(4)				
O(2)^i−Sn(1)−O(3)	78.3(3)	O(1)−Sn(2)−O(6)	97.0(3)	O(4)^i−Sn(2)−C(5)	108.3(6)	O(10)−Sn(6)−C(21)	97.7(4)				
O(1)^i−Sn(1)−O(4)	77.6(3)	O(2)^i−Sn(3)−O(5)^i	98.0(3)	O(5)^i−Sn(2)−C(5)	108.6(5)	$\langle O-Sn_o-C\rangle_c$	98.0				
O(1)−Sn(2)−O(4)^i	77.6(3)	$\langle O-Sn_p-O\rangle_t$	137.7	O(6)−Sn(2)−C(5)	112.6(5)	O(3)−Sn(4)−C(13)	96.9(5)				
O(4)^i−Sn(2)−O(5)^i	77.9(3)	O(2)^i−Sn(1)−O(4)	137.6(3)	O(2)^i−Sn(3)−C(9)	109.8(5)	O(6)−Sn(4)−C(13)	97.7(5)				
O(5)^i−Sn(2)−O(6)	78.6(3)	O(1)^i−Sn(1)−O(3)	137.8(3)	O(3)−Sn(3)−C(9)	110.4(5)	O(1)−Sn(5)−C(17)	98.0(6)				
O(2)^i−Sn(3)−O(3)	78.2(3)	O(1)−Sn(2)−O(5)^i	137.3(3)	O(5)^i−Sn(3)−C(9)	110.0(5)	O(2)−Sn(5)−C(17)	99.3(5)				
O(3)−Sn(3)−O(6)	77.8(3)	O(4)^i−Sn(2)−O(6)	137.6(3)	O(6)−Sn(3)−C(9)	110.8(5)	O(4)−Sn(6)−C(21)	98.4(4)				
O(5)^i−Sn(3)−O(6)	78.2(3)	O(3)−Sn(3)−O(5)^i	138.2(3)			O(5)−Sn(6)−C(21)	97.8(5)				
		O(2)^i−Sn(3)−O(6)	137.9(3)	$\langle O-Sn_o-C\rangle_t$	173.0	$\langle Sn_p-O-Sn_p\rangle$	101.6				
$\langle O-Sn_o-OH\rangle_c$	90.4	$\langle O-Sn_o-OH\rangle_c$	77.6	O(7)−Sn(4)−C(13)	173.1(5)	Sn(1)^i−O(1)−Sn(2)	102.3(3)				
O(3)−Sn(4)−O(8)	87.4(3)	O(7)−Sn(4)−O(8)	75.6(3)	O(7)−Sn(5)−C(17)	173.0(6)	Sn(1)^i−O(2)−Sn(3)^i	101.7(3)				
O(6)−Sn(4)−O(9)	93.6(3)	O(7)−Sn(4)−O(9)	79.4(3)	O(7)−Sn(6)−C(21)	172.9(4)	Sn(1)−O(3)−Sn(3)	101.6(3)				
O(1)−Sn(5)−O(9)	93.3(3)	O(7)−Sn(5)−O(9)	79.7(3)			Sn(1)−O(4)−Sn(2)^i	101.8(3)				
O(2)−Sn(5)−O(10)	88.0(3)	O(7)−Sn(5)−O(10)	75.7(3)			Sn(2)^i−O(5)−Sn(3)^i	101.4(3)				
O(4)−Sn(6)−O(8)	89.7(3)	O(7)−Sn(6)−O(8)	77.8(3)			Sn(2)−O(6)−Sn(3)	101.1(3)				
O(5)−Sn(6)−O(10)	90.2(3)	O(7)−Sn(6)−O(10)	77.5(3)	$\langle Sn_p-O-Sn_o\rangle$	103.3	$\langle Sn_p-O-Sn_o\rangle$	133.6				
$\langle O-Sn_o-O\rangle_c$	75.5	$\langle HO-Sn_o-OH\rangle_c$	99.0	Sn(1)^i−O(1)−Sn(5)	103.4(3)	Sn(2)−O(1)−Sn(5)	133.0(4)				
O(3)−Sn(4)−O(6)	75.3(3)	O(8)−Sn(4)−O(9)	98.9(3)	Sn(1)^i−O(2)−Sn(5)	103.7(3)	Sn(3)^i−O(2)−Sn(5)	135.0(4)				
O(1)−Sn(5)−O(2)	74.8(3)	O(9)−Sn(5)−O(10)	99.0(3)	Sn(3)−O(3)−Sn(4)	103.0(3)	Sn(1)−O(3)−Sn(4)	135.0(4)				
O(4)−Sn(6)−O(5)	76.5(3)	O(8)−Sn(6)−O(10)	99.2(3)	Sn(2)^i−O(4)−Sn(6)	102.4(3)	Sn(1)−O(4)−Sn(6)	132.9(4)				
$\langle O-Sn_o-O\rangle_c$	87.0	$\langle O-Sn_o-OH\rangle_t$	159.6	Sn(2)^i−O(5)−Sn(6)	103.2(3)	Sn(3)^i−O(5)−Sn(6)	132.5(4)				
O(3)−Sn(4)−O(7)	84.6(3)	O(6)−Sn(4)−O(8)	158.1(3)	Sn(3)−O(6)−Sn(4)	103.9(3)	Sn(2)−O(6)−Sn(4)	133.1(4)				
O(6)−Sn(4)−O(7)	89.2(3)	O(3)−Sn(4)−O(9)	160.6(3)	$\langle Sn_o-O-Sn_o\rangle$	102.5	$\langle Sn_o-OH-Sn_o\rangle$	102.1				
O(1)−Sn(5)−O(7)	88.7(3)	O(2)−Sn(5)−O(9)	160.5(3)	Sn(4)−O(7)−Sn(6)	105.0(3)	Sn(4)−O(8)−Sn(6)	101.6(3)				
O(2)−Sn(5)−O(7)	84.5(3)	O(1)−Sn(5)−O(10)	157.9(3)	Sn(4)−O(7)−Sn(5)	97.8(3)	Sn(4)−O(9)−Sn(5)	102.5(3)				
O(4)−Sn(6)−O(7)	87.4(3)	O(4)−Sn(6)−O(10)	160.3(3)	Sn(5)−O(7)−Sn(6)	104.7(3)	Sn(5)−O(10)−Sn(6)	102.2(3)				
O(5)−Sn(6)−O(7)	87.6(3)	O(5)−Sn(6)−O(8)	160.4(3)	$\langle Sn_p-C-C\rangle$	114.3	$\langle Sn_o-C-C\rangle$	117.4				
$\langle O-Sn_p-C\rangle_c$	110.3	$\langle HO-Sn_o-C\rangle_c$	98.3	Sn(1)−C(1)−C(2)	118.4(13)	Sn(4)−C(13)−C(14)	115.6(11)				
O(1)^i−Sn(1)−C(1)	107.6(5)	O(8)−Sn(4)−C(13)	97.7(5)	Sn(2)−C(5)−C(6)	111.1(11)	Sn(5)−C(17)−C(18)	121.6(15)				
O(2)^i−Sn(1)−C(1)	110.3(5)	O(9)−Sn(4)−C(13)	100.4(5)	Sn(3)−C(9)−C(10)	113.4(10)	Sn(6)−C(21)−C(22)	115.0(9)				
O(3)−Sn(1)−C(1)	113.2(5)	O(9)−Sn(5)−C(17)	97.6(6)								

[a] $\langle\ \rangle$: average values. Subscripts p and or refer to five- and six-coordinate tin atoms, respectively. [b] Subscripts c and t refer to cis and trans positions, respectively.

bridges which exchange hydrogen bonds with the isopropyl alcohol molecules are those which are not hydrogen bonded to the hydroxyl counterions. This complex network of hydrogen bonds is characterized by an average O−O distance of 2.74 Å (Figure 1 and Table 3).

^{119}Sn Solution NMR. ^{119}Sn {^{1}H} NMR spectra of **C1** and **P2**, dissolved in C_6D_6 or CD_2Cl_2, are identical. Figure 2 presents the ^{119}Sn {^{1}H} NMR spectrum of **P2** in C_6D_6. Two resonances are observed at −280.1 and −447.4 ppm, corresponding to five- and six-coordinate monoalkyltin species, respectively.[36] Each resonance exhibits satellites related to two bond (oxo and hydroxo bridges) scalar couplings between tin atoms of different or identical coordination (Table 4).[9,13,37] Integration, performed on non-^{1}H-decoupled spectra, indicates an equal amount of five- and six-coordinate tin atoms.

Moreover, the ^{119}Sn {^{1}H} NMR spectra of solutions **S2** and **S3** show the same two resonances and coupling features, just after preparation, about 15 min after hydrolysis, which was the minimum time to record a ^{119}Sn {^{1}H} NMR spectrum with an acceptable signal to noise ratio. Two and three bond J_{Sn-H} coupling constants were also determined from non-^{1}H-decoupled spectra. They depend on tin coordination: $^2J_{Sn_o-H}$ = 105 Hz,

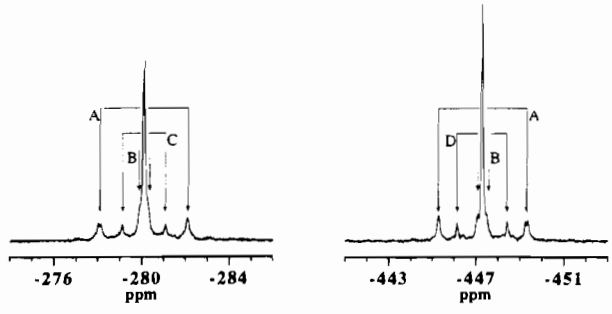

Figure 2. ^{119}Sn {^{1}H} NMR spectrum of **P2** dissolved in C_6D_6 (subscripts p and o refer to five- and six-coordinate tin atoms, respectively): $A = {}^2J^{119}Sn_o-{}^{119/117}Sn_p$ (single oxo bridge); $B = {}^2J^{119}Sn_o-{}^{119/117}Sn_p$ (double oxo bridge); $C = {}^2J^{119}Sn_p-{}^{117}Sn_p$ (double oxo bridge); $D = {}^2J^{119}Sn_o-{}^{117}Sn_o$ (double oxo-hydroxo bridge).

(36) Harris, R. K.; Kennedy, J. D.; McFarlane, W. *NMR and the Periodic Table*; Academic Press: London, England, 1978; p 348.
(37) Lockhart, T. P.; Puff, H.; Schuh, W.; Reuter, H.; Mitchell, T. N. *J. Organomet. Chem.* **1989**, *366*, 61.

Table 4. J^2_{Sn-Sn} Values for $\{(BuSn)_{12}(\mu_3\text{-}O)_{14}(\mu_2\text{-}OH)_6\}(OH)_2$

isotope and environment[a]	paths[b]	⟨Sn−Sn⟩,[c] Å	$\lvert J^2_{Sn-Sn}\rvert$, Hz
$^{119}Sn_p-^{119/117}Sn_o$ or $^{119}Sn_o-^{119/117}Sn_p$	single oxo bridge	3.83	383/366
$^{119}Sn_p-^{119/117}Sn_o$ or $^{119}Sn_o-^{119/117}Sn_p$	double oxo bridge	3.31	40/38[d]
$^{119}Sn_p-^{117}Sn_p$	double oxo bridge	3.18	177
$^{119}Sn_o-^{117}Sn_o$	double oxo−hydroxo bridge	3.26	205

[a] Subscripts p and o are relative to five- and six-coordinate tin atoms, respectively. [b] See discussion. [c] Average tin−tin distance related to a peculiar two bonds path. [d] Splitting not experimentally observed.

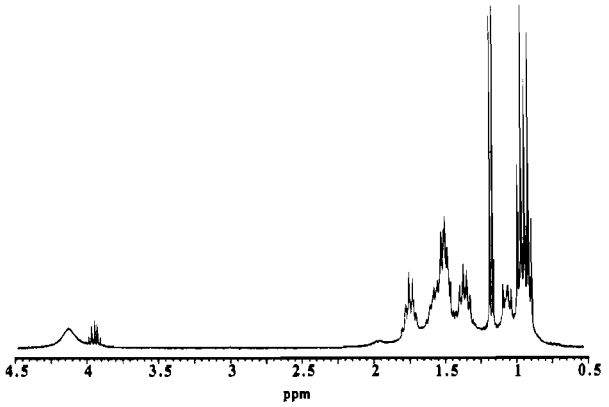

Figure 3. ^1H NMR spectrum of **P2** dissolved in CD_2Cl_2.

$J^3_{Sn_o-H}$ = 105 Hz, $J^2_{Sn_p-H}$ = 99 Hz, and $J^3_{Sn_p-H}$ = 145 Hz. Attribution of the larger coupling value to J^3 was made according to literature.[38] J^n_{Sn-H} with n greater than 3 were not observed.

^1H and ^{13}C Solution NMR. ^1H NMR spectrum of **C1** and **P2** in CD_2Cl_2 have the same general features (Figure 3). All of the resonances associated with butyl chains and the doublet due to the methyl groups of isopropyl alcohol (1.15 ppm) are found between 0.8 and 2.2 ppm. The septuplet related to the methyne of isopropyl alcohol is located at 3.95 ppm. A broad resonance is also observed around 4.2 ppm and was attributed to OH groups with their protons experiencing intermediate exchange. Integrations over these three regions (OH, methyne, and 0.8−2.2 ppm) were performed for **C1** and **P2**. For **C1** they are in perfect agreement with the formula $\{(BuSn)_{12}O_{14}(OH)_6\}(OH)_2(HOPr^i)_4$ obtained from the structure determination. For **P2**, integrations indicate a ratio, Butyl/OPr^i = 12/2.

Complete assignment, between 0.8 and 2.2 ppm, was not directly possible because of overlapped resonances. Anyhow, two types of terminal methyl groups of the butyl chains are clearly observed in the high-field region.

Because of its lower content of isopropyl alcohol and its identical ^{119}Sn, ^1H, and ^{13}C solution NMR features, **P2** was used for all of the 2D NMR experiments. The $^1H-^1H$ COSY[31] spectrum of **P2** in CD_2Cl_2 is presented in Figure 4. Starting from the triplets of the terminal methyl groups, the resonances of two different butyl chains can be located (Table 5).

^{13}C NMR spectra of **C1**, $\{(BuSn)_{12}(\mu_3\text{-}O)_{14}(\mu_2\text{-}OH)_6\}(OH)_2(HOPr^i)_4$, and **P2** show a better resolution. They clearly exhibit the splitting of every resonance of the butyl chains (Figure 5). Small satellites, related to scalar coupling between tin and carbon, allow measurement $J^n_{^{119/117}Sn-^{13}C}$ for $1 \le n \le 3$ (Table 5).

A $^{13}C-^1H$ heteronuclear shift correlated NMR[30] experiment performed on **P2** (Figure 6) has allowed assignment of, without ambiguity, all of the resonances observed in the ^{13}C NMR spectra (Table 5).

Two Dimensional $^{119}Sn-^1H$ Correlation Spectroscopy. The complex ^1H NMR spectrum, with overlapped resonances, did not allow clear spotting of all the $^{119/117}Sn$ coupling satellites. Therefore, a 2D $^{119}Sn-^1H$ correlation spectroscopy experiment was performed with an evolution time of 4.5 ms ($^1/_2J$ with $J \approx$ 110 Hz) allowing one to trace the relations between tin atoms and the two first CH_2 groups of both types of butyl chains. The $^{119}Sn-^1H$ heteronuclear shift correlated NMR[30] spectrum of compound **P2**, dissolved in CD_2Cl_2, is presented in Figure 7. The simple pattern obtained clearly shows that the five-coordinate tin atoms are correlated to the CH_2 located at 1.48 and 1.74 ppm in the ^1H NMR spectra, and the six-coordinate tin atoms are correlated to the CH_2 located at 1.025 and 1.564 ppm. This final observation has allowed complete assignment of all of the ^1H and ^{13}C NMR resonances of $\{(BuSn)_{12}O_{14}(OH)_6\}(OH)_2$, which are reported in Table 5.

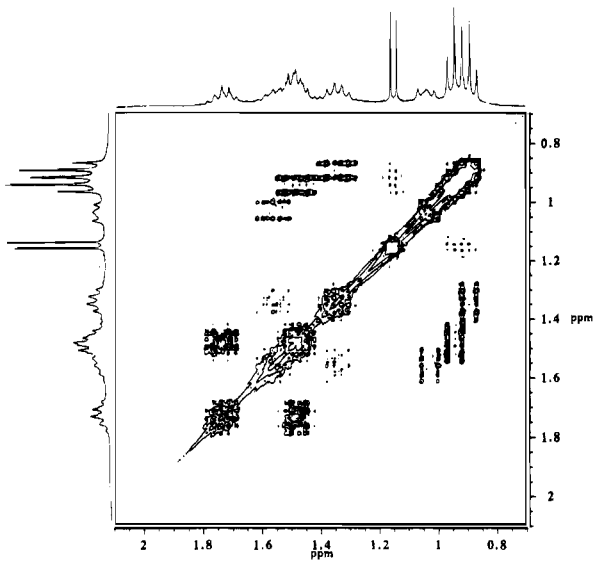

Figure 4. $^1H-^1H$ COSY NMR spectrum of **P2** dissolved in CD_2Cl_2.

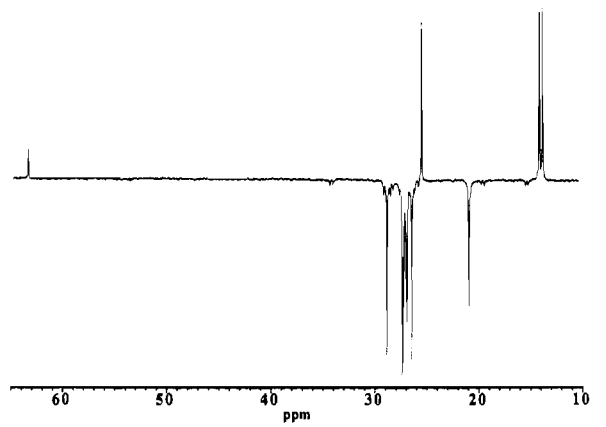

Figure 5. ^{13}C INEPT refocused and decoupled NMR spectrum of **P2** dissolved in CD_2Cl_2 (CH_3 and CH positive, CH_2 negative).

^{119}Sn Solid State NMR Spectroscopy. The ^{119}Sn MAS NMR spectra of **C1** and **P2** are displayed in Figure 8. For each compound, two patterns of isotropic bands, located around −280 and −450 ppm, are easily assigned, from ^{119}Sn solution NMR

(38) Lycka, A.; Jirman, J.; Holecek, *J. Magn. Reson. Chem.* **1991**, *29*, 1212.

Table 5. ^{1}H and ^{13}C NMR Data of $\{(BuSn)_{12}(\mu_3\text{-}O)_{14}(\mu_2\text{-}OH)_6\}(OH)_2$

$\delta(^{1}H)$,[a] ppm	J^{3}_{H-H},[a] Hz	$\delta(^{13}C)$, ppm	J^{n}_{C-Sn}, Hz	assgnmt[b]
(1.48)	(7.8, tr)	20.9	$^{119}867-^{117}829$	$Sn_p-\underline{CH_2}-CH_2-CH_2-CH_3$
1.02	8.4,[c]	26.8	$^{119}1136-^{117}1086$	$Sn_o-\underline{CH_2}-CH_2-CH_2-CH_3$
1.74	7.5, q	27.2	47	$Sn_p-\overline{CH_2}-\underline{CH_2}-CH_2-CH_3$
1.56	(8.3, q)	28.6	49	$Sn_o-CH_2-\overline{CH_2}-\underline{CH_2}-CH_3$
(1.48)	(7.3, sext)	26.3	96	$Sn_p-CH_2-\overline{CH_2}-\underline{CH_2}-CH_3$
1.34	7.3, sext	27.0	156	$Sn_o-CH_2-CH_2-\overline{CH_2}-\underline{CH_3}$
0.94	7.4, tr	13.6	<5	$Sn_p-CH_2-CH_2-\overline{CH_2}-\underline{CH_3}$
0.90	7.3, tr	13.9	<5	$Sn_o-CH_2-CH_2-CH_2-\underline{\overline{CH_3}}$
4.2				*OH*

[a] Values in parentheses are less accurate due to overlapped resonances. Abbreviations: tr = triplet, q = quintet, sext = sextet. [b] Sn_p and Sn_o refer to five- and six-coordinate tin atoms, respectively. [c] Actually not a real triplet. See discussion.

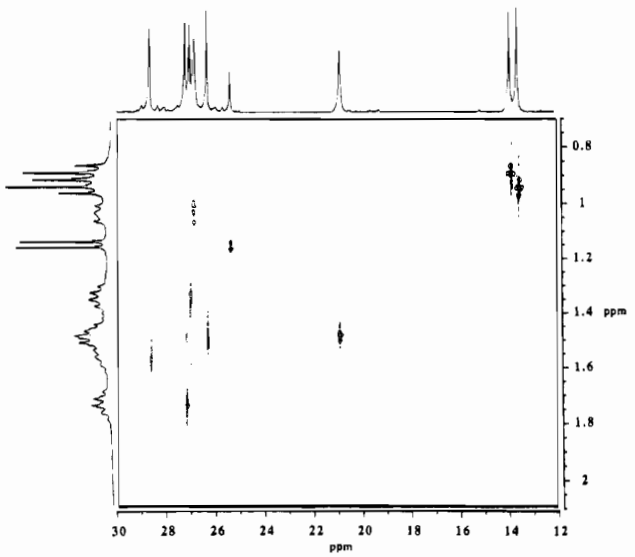

Figure 6. $^{13}C-^{1}H$ heteronuclear shift correlated 2D NMR spectrum of **P2** dissolved in CD_2Cl_2.

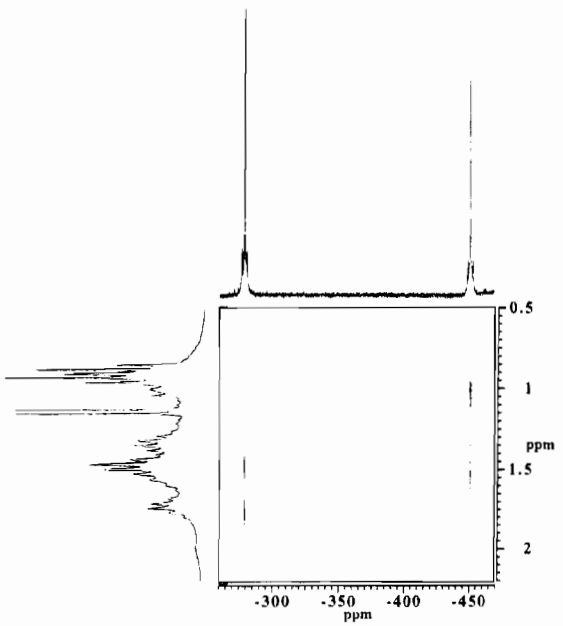

Figure 7. $^{119}Sn-^{1}H$ heteronuclear shift correlated 2D NMR spectrum of **P2** dissolved in CD_2Cl_2.

data and literature,[32] to five- and six-coordinate monoalkyltin, respectively. Two five-coordinate and two six-coordinate tin atoms were necessary to simulate the isotropic bands of **C1**. Isotropic bands of **P2** are broader and exhibited a more complex structure (three types of five-coordinate tin atoms and four types of six-coordinate tin atoms). By iterative adjustment of the spinning side bands (Figure 8), the tensorial components of

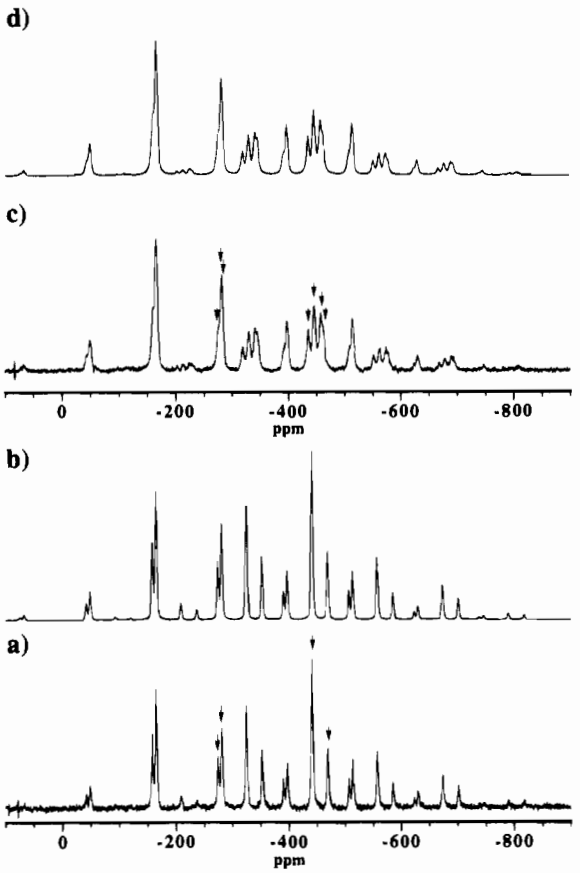

Figure 8. ^{119}Sn MAS NMR spectrum of **C1** (a) and simulated spectrum (b). ^{119}Sn MAS NMR spectrum of **P2** (c) and simulated spectrum (d). Isotropic bands are indicated with arrows (rotation speed = 13 000 Hz).

^{119}Sn shielding were determined for each type of tin atoms of each compound. For both compounds, relative intensities of five- and six-coordinate tin atoms are roughly in a 1:1 ratio. Results are summarized in Table 6.

Discussion

The ^{119}Sn solution NMR results show that the same oligomer is obtained upon hydrolysis of $BuSn(OPr^{i})_3$ and $BuSn(OAm^{t})_3$ with more than three water molecules per tin atom. This oligomer is characterized by two ^{119}Sn resonances at −280.1 and −447.4 ppm, and four J^{2}_{Sn-Sn} scalar coupling constants (Figure 2 and Table 4). According to the molecular structure determined for **C1** (Figure 1), the entity, characterized in solution, corresponds to $\{(BuSn)_{12}O_{14}(OH)_6\}(OH)_2$. This formula, which includes the hydroxyl counterions, is justified by comparison with other ^{119}Sn NMR results. Recently, $\{(BuSn)_{12}O_{14}(OH)_6\}Cl_2(H_2O)_2$, which exhibits the same oxo−hydroxo butyltin core structure, was reported to give two ^{119}Sn

Table 6. ^{119}Sn Shielding Tensorial Values and Related Information

no.	δ_{iso}, ppm	δ_A,[a] ppm	η[a]	σ_{11}, ppm	σ_{22}, ppm	σ_{33}, ppm	intens[b]	coord
				C1				
1	−274.6	360.2	0.25	49.4	139.5	634.8	2.0	5
2	−281.4	360.2	0.30	47.2	155.3	641.7	3.7	5
3	−441.5	278.9	0.40	246.2	357.8	720.4	4.3	6
4	−469.4	313.8	0.25	273.3	351.7	783.2	2.0	6
				P2				
1′	−276.1	372.0	0.30	34.3	145.9	648.1	2.0	5
2′	−281.1	372.0	0.35	30.0	160.2	653.1	2.3	5
3′	−283.5	360.0	0.10	85.5	121.5	643.5	2.1	5
4′	−435.7	267.3	0.50	235.2	368.9	703.0	1.0	6
5′	−446.2	267.3	0.35	265.8	359.3	713.5	1.8	6
6′	−457.6	290.6	0.40	254.2	370.4	748.2	1.8	6
7′	−462.3	313.8	0.05	297.6	313.2	776.1	1.0	6

[a] $\sigma_{iso} = -\delta_{iso} = (\sigma_{11} + \sigma_{22} + \sigma_{33})/3$; $\delta_A = \sigma_{33} - \sigma_{iso}$; $\eta = |\sigma_{22} - \sigma_{11}|/|\sigma_{33} - \sigma_{iso}|$ with $|\sigma_{33} - \sigma_{iso}| > |\sigma_{11} - \sigma_{iso}| > |\sigma_{22} - \sigma_{iso}|$. [b] Intensities were normalized to 12 for each compound.

resonances at −283.1 and −468.1 ppm, in CD_2Cl_2.[9] Likewise, the compound $\{(BuSn)_{12}O_{14}(OH)_6\}(O_2CCH_3)_2$, which is prepared by reacting 1 mol of $\{(BuSn)_{12}O_{14}(OH)_6\}(OH)_2$ with 2 mol of acetic acid, gives, in CD_2Cl_2, two ^{119}Sn chemical shifts at −281 and −457 ppm.[39] All of these different values clearly indicate that in solvents with low dielectric constant, such as benzene, dichloromethane, and alcohol ($HOPr^i$ and $HOAm^t$), the anions stay in the vicinity of the macro-cation and therefore influence the chemical shifts of tin atoms, especially six-coordinate ones. The observation, for $\{(BuSn)_{12}O_{14}(OH)_6\}(OH)_2$, of a single resonance for each type of tin coordination also shows that the unequivalence found among the five- or six-coordinate tin atoms, in the molecular structure of **C1**, is removed in solution. The hydroxyl counterions (O(13)), which are hydrogen bonded to a peculiar μ_2-OH (O(9), Figure 1) in **C1**, probably undergo in solution a fast delocalization on all the bridging hydroxy groups on the time scale of ^{119}Sn NMR. This comment on the delocalization of the counterions also applies for $\{(BuSn)_{12}O_{14}(OH)_6\}Cl_2(H_2O)_2$ and $\{(BuSn)_{12}O_{14}(OH)_6\}(O_2CCH_3)_2$.[9,39]

The compound formed upon hydrolyzing butyltin alkoxide is derived from the oxo−hydroxo monoorganotin macro-cation, $\{(RSn)_{12}O_{14}(OH)_6\}^{2+}$, which has already been obtained in the base hydrolysis of $RSnCl_3$ (R = isopropyl or butyl). Yet, in these studies, the positive charges were always compensated for by two chloride ions.[7,9] The reason why a cationic cluster is formed is not clear but is probably related to the stability of the trimeric unit "$[(BuSn)_3(\mu_3\text{-}O)(\mu_2\text{-}OH)_3]$", which is also encountered in the reaction product of butylstannonic acid with diphenylphosphinic acid, $\{[BuSn(OH)O_2PPh]_3O\}(O_2PPh)$.[3] For comparison, a dodecameric cluster, $Ti_{12}O_{16}(OPr^i)_{16}$ has been obtained by hydrolysis of titanium isopropoxide.[40] This cluster, which exhibits a molecular structure very similar to the one of $\{(RSn)_{12}O_{14}(OH)_6\}^{2+}$, is on the contrary neutral.

According to ^{1}H NMR results, the precipitate **P2** used in this work corresponds to the stoichiometry $\{(BuSn)_{12}O_{14}(OH)_6\}(OH)_2(HOPr^i)_x$ with $x \approx 2$. Yet, **P2** loses easily its isopropyl alcohol molecules to yield a solid of formula $\{(BuSn)_{12}O_{14}(OH)_6\}(OH)_2$, which is insoluble in benzene and dichloromethane. Precipitates, such as **P2**, obtained by hydrolyzing ($H_2O/Sn > 3$) liquid $BuSn(OPr^i)_3$ with water diluted in isopropyl alcohol (10 wt % of H_2O), might correspond to the stoichiometry of **C1** ($HOPr^i/Sn = 1/3$) when standing in their mother liquor but undergo fast drying in air because of their fine granulometry. Or, they might exhibit, from the beginning, another or no defined stoichiometry. This point is not clear, but, as long as they have not lost all their isopropyl alcohol molecules, they can be considered as practical, quickly prepared, soluble, and good yield (>50%) sources of $\{(BuSn)_{12}O_{14}(OH)_6\}(OH)_2$.

In the ^{119}Sn solution NMR of $\{(BuSn)_{12}O_{14}(OH)_6\}(OH)_2$ (Figure 2), the shift of 166.3 ppm toward high field upon increasing the coordination number of tin by one fits in the usual range of 150−200 ppm.[36] This variation of the shielding constant, upon the addition of an oxygen atom in the coordination of tin, cannot be accounted only by a diamagnetic effect, since the electronegativity of oxygen would predict a shift in the opposite direction.[36] Therefore, the variation of the shielding constant is more related to a paramagnetic effect. In such a case, $\sigma_{para} \approx \langle r^{-3}\rangle/\Delta E$, with r being the distance of an electron to the nucleus, what reflects the bond length around tin, and ΔE the energy difference between the ground state and the first excited state.[36] Assuming that ΔE does not change too much between five- and six-coordinate tin atoms, an increase in the average bond length around tin atoms yields, through a decrease of $\langle r^{-3}\rangle$, to an increase of the paramagnetic contribution to the shielding constant, and therefore to a shift of the resonance toward high field. Such observation agrees quite well with the variation of the average distances around each type of tin atoms determined in the molecular structure of $\{(BuSn)_{12}(\mu_3\text{-}O)_{14}(\mu_2\text{-}OH)_6\}(OH)_2(HOPr^i)_4$, $\langle Sn_p\text{−}X\rangle = 2.07$ Å and $\langle Sn_o\text{−}X\rangle = 2.12$ Å (Table 3).

The observation of the four coupling constants (Table 4) in the ^{119}Sn solution NMR spectrum of $\{(BuSn)_{12}O_{14}(OH)_6\}(OH)_2$ (Figure 2) also agrees with the molecular structure determined on $\{(BuSn)_{12}(\mu_3\text{-}O)_{14}(\mu_2\text{-}OH)_6\}(OH)_2(HOPr^i)_4$. The two bond tin−tin connections in the Sn−O−Sn framework of **C1** can be described as follows for each type of tin coordination (atom X^i is the symmetric of atom X by the inversion center located at the center of the macro-cation, Figure 1):

(i) A five-coordinate tin atom is connected to two other five-coordinate tin atoms through double oxo bridges (i.e., Sn(3) to Sn(1) through O(3) and $O(2)^i$ and to Sn(2) through O(6) and $O(5)^i$). A five-coordinate tin atom is also connected to one six-coordinate tin atom through a double oxo bridge (i.e., Sn(3) to Sn(4) through O(3) and O(6)). Finally, a five-coordinate tin atom is connected to two six-coordinate tin atoms through single oxo bridges (Sn(3) to $Sn(5)^i$ through $O(2)^i$ and to $Sn(6)^i$ through $O(5^i)$).

(ii) A six-coordinate tin atom is connected to two other six-coordinate tin atoms through double oxo−hydroxo bridges (i.e., Sn(4) to Sn(5) through O(7) and O(9) and to Sn(6) through O(7) and O(8). A six-coordinate tin atom is also connected to one five-coordinate tin atom through a double oxo bridge (i.e., Sn(4) to Sn(3) through O(3) and O(6)). Finally, a six-coordinate tin atom is connected to two five-coordinate tin atoms through a single oxo bridge (i.e., Sn(4) to Sn(1) through O(3) and to Sn(2) through O(6)).

Therefore, four different two bond connections are found in **C1**: one two bond path (double oxo bridge) between two five-coordinate tin atoms, one two bond path (double oxo−hydroxo bridge) between two six-coordinate tin atoms, and two different two bond paths (single or double oxo bridge) between two tin atoms of different coordination. From intensity considerations, the larger intersite coupling constant is unambiguously assigned to single oxo bridge connections, while the smaller intersite coupling constant is related to double oxo bridges (Table 4 and Figure 2). There seems to be no straightforward relation between the scalar coupling constant and the average tin−tin

(39) Ribot, F.; Banse, F.; Diter, F.; Sanchez, C. *New. J. Chem.* **1995**, *19*, 1163.
(40) Day, V. W.; Eberspacher, T. A.; Klemperer, W. G.; Park, C. W. *J. Am. Chem. Soc.* **1993**, *115*, 8469.

distance. Lockhart et al. have experimentally established, on several hexaorganodistannoxanes ($R_3Sn-O-SnR'_3$), a linear relation between the Sn−O−Sn angle and the $J^2_{^{119}Sn,^{119}Sn}$ value.[37] Only the intersite scalar coupling values in $\{(BuSn)_{12}O_{14}(OH)_6\}(OH)_2$ seem to agree with this relation. It is probable that in such a complex framework of Sn−O bonds, the $J^2_{Sn,Sn}$ values, which reflect the s-character in the bonding orbitals, depend in a complex way on Sn−Sn distances and Sn−O−Sn angles.

It is also interesting to note that the center of the outside components, only related to the ^{119}Sn isotope, of the larger intersite coupling is always shifted from the central resonance. This shift can be attributed to a small second order effect. Its experimental determination (≈4 Hz) agrees, within the digital resolution, with its theoretical value of 2.5 Hz, calculated from the scalar coupling constant (383 Hz) and the separation between the resonances of tin atoms in five and six coordination (15 511 Hz).[41]

One and two dimensional NMR experiments clearly show that all the ^1H and ^{13}C resonances of the butyl chains are split in two groups, directly related to the two coordinations that tin atoms exhibit in $\{(BuSn)_{12}O_{14}(OH)_6\}(OH)_2$ (Table 5). Both types of butyl chain exhibit the same ^1H and ^{13}C chemical shift sequences: $(CH_3)^4 < (CH_2)^1 \leq (CH_2)^3 < (CH_2)^2$ (1 being the closest to tin atoms). Both groups also exhibit the same, generally found, scalar coupling sequence: $J^1_{Sn,C} \gg J^3_{Sn,C} > J^2_{Sn,C}$. Yet, odd bond paths scalar coupling greatly depend on the coordination of tin, being larger for six-coordinate atoms.[38] These results show that the coordination of tin is felt, through chemical bond, up to the third carbon atom of the butyl chains at least. The splitting of the ^1H and ^{13}C NMR signals of the methyl end groups is likely also due to tin coordination, but geometrical effects, related to the location of five- and six-coordinate tin atoms in the cluster (Sn_o at each end and close to the μ_2-OH), cannot be ruled out.

The ^1H NMR resonance (1.02 ppm) of the CH_2 groups closer to the six-coordinate tin atoms does not exhibit the characteristic shape of a triplet (Figure 3). This feature can be attributed to a AA′ system for this CH_2.

In the case of the chloride analogue of the cluster, $\{(BuSn)_{12}O_{14}(OH)_6\}Cl_2$, in methanol, Dakternieks et al. have observed, upon aging, the replacement of some of the bridging hydroxy by methoxy groups.[9] This reaction does not seem to happen with isopropyl alcohol and $\{(BuSn)_{12}O_{14}(OH)_6\}(OH)_2$, since the ^{119}Sn NMR chemical shift of six-coordinate tin atoms does not show any evolution with time. Moreover, the ^1H and ^{13}C NMR signals attributed to isopropyl groups for **C1** and **P2** always correspond to free isopropyl alcohol.

The ^{119}Sn MAS NMR spectrum of **C1** shows several five- and six-coordinate tin atoms (Figure 8 and Table 6). Their relative proportions are roughly 1:1. Each type of tin coordination gives rise to two resonances with a ratio of 1:2. If accidental overlapping, which would have to occur for both coordinations of tin, are neglected, the ratio 1:2 indicates that for ^{119}Sn MAS NMR the symmetry of **C1** is apparently higher than for X-ray diffraction. Actually, distances and angles (Table 3) show that among six-coordinate tin atoms, Sn(6) is clearly different from Sn(4) and Sn(5), which are the two tin atoms connected through the μ_2-OH (O(9)) hydrogen bond to the hydroxyl counterions (O(13)). Moreover, considering only the Sn−O−Sn framework, the molecular structure of **C1** exhibits, in addition to the inversion center seen by X-ray diffraction, a pseudo-mirror plane (Figure 9). This pseudo-mirror which goes

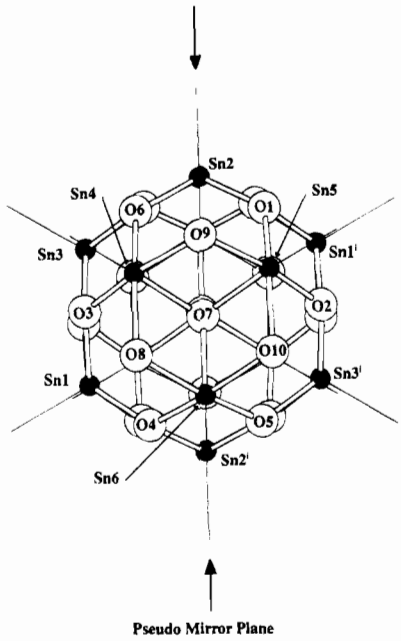

Figure 9. Molecular drawing of $\{(BuSn)_{12}O_{14}(OH)_6\}^{2+}$ (from the structure of **C1**) showing the pseudo-mirror plane. Superscript i refers to the symmetric by the inversion center located at the center of the cluster. Hydrogen and carbon atoms have been removed for clarity.

through Sn(6), O(9), and Sn(2), makes Sn(4) and Sn(5) almost equivalent, as well as Sn(1) and Sn(3^i)^i. Therefore, according to these symmetry considerations and to NMR integrations, site no. 3 (−441.5 ppm) can be attributed to Sn(4) and Sn(5), site no. 4 (−469.4 ppm) can be assigned to Sn(6), site no. 1 to Sn(2), and finally site no. 2 to Sn(1) and Sn(3). This apparent symmetry in ^{119}Sn MAS NMR (inversion center and mirror plane) is yet lower than the one observed in solution (ternary axis going through O(7) and O(7^i)). This feature is related to the hydrogen bonding of the hydroxyl counterions (O(13)) to a specific hydroxy bridge (O(9)) in the solid compound. It results that Sn(4)−Sn(5) (3.178 Å) is much shorter than Sn(4)−Sn(6) (3.302 Å) and Sn(5)−Sn(6) (3.298 Å).

Averages of the isotropic chemical shifts, weighted by their site integration, for five- and six-coordinate tin atoms give −279.2 and −450.8 ppm, respectively. These values match quite well the solution ^{119}Sn NMR results obtained for $\{(BuSn)_{12}O_{14}(OH)_6\}(OH)_2$. The solubilization of $\{(BuSn)_{12}O_{14}(OH)_6\}(OH)_2(HOPr^i)_4$ seems to cause only the relaxation of geometrical constraints encountered in the solid state, such as the localization of the hydroxyl counterions (O(13)) on a specific bridging hydroxy group (O(9)). Indeed, the isotropic chemical shifts of six-coordinate tin atoms are more spread in the solid state than the ones of five-coordinate tin atoms.

Relatively few ^{119}Sn shielding tensorial properties are reported in the literature for monoalkyltin compounds, and therefore a precise discussion of the anisotropies and asymmetries is quite complex. Moreover, it is most of the time impossible to find simple relations between the principal axis system of the shielding tensor and the molecular axis of tin atoms.[42] Yet, the following comments can be made for ^{119}Sn tensorial properties of $\{(BuSn)_{12}O_{14}(OH)_6\}(OH)_2(HOPr^i)_4$. Anisotropy ($\delta_A$) are larger for five-coordinate tin atoms than for six-coordinate ones,[32] as expected from their local geometry. Asymmetries (η) for both types of coordination show similar values, which correspond to rhombic symmetry. Such results could be expected from the coordination polyhedra of tin atoms

(41) Canet, D. *La RMN Concepts et Méthodes*; InterEditions: Paris, France, 1991; p 62.

(42) Klaus, E.; Sebald, A. *Magn. Reson. Chem.* **1994**, *32*, 679.

which are distorted square pyramids for "$CSnO_4$" and pseudo-octahedras for "$CSnO_5$". Sites no. 1 and no. 2 exhibit identical anisotropies and asymmetries, within the analysis accuracy, showing that they have almost similar environments. Indeed, the main difference between sites no. 1 and no. 2 comes from their second neighbors and the way they are linked to them. The variation of the anisotropies of sites no. 3 and no. 4 is more likely related to the peculiar role played by O(9), which is only bound to tin atoms belonging to site no. 3.

The ^{119}Sn MAS NMR spectrum of **P2** (Figure 8) show more sites than for **C1**, but the relative ratio of five- to six-coordinate tin atoms remains around 1 (Table 6). As in **C1**, the averages of the isotropic chemical shifts, weighted by their site integration, for five- and six-coordinate tin atoms give values (−280.3 and −450.9 ppm, respectively) which are in very good agreement with the solution ^{119}Sn chemical shifts of $\{(BuSn)_{12}O_{14}(OH)_6\}(OH)_2$. The differences between **C1** and **P2** are likely related to the difference in their OPr^i/Sn ratio. Removing in **C1** some of the isopropyl alcohol molecules, originally linked to the hydroxo bridges (O(8) or O(10)), creates new and slightly different tin environments, especially for six-coordinate tin atoms. The general comments made for the ^{119}Sn shielding tensorial properties of **C1** remains valid for **P2**. Anyhow, the overlapping of the resonances in the ^{119}Sn MAS NMR spectrum of **P2** might yield a less accurate analysis of the amplitudes of the spinning side bands and therefore less reliable tensorial properties. This problem might explain why the asymmetry parameters (η) are more spread (from 0.05 to 0.5) than those previously determined for **C1**.

Conclusion

Hydrolysis of butyltin trialkoxides with more than three water molecules per tin yields the cagelike oxo−hydroxo butyltin cluster, $\{(BuSn)_{12}O_{14}(OH)_6\}(OH)_2$. Its molecular structure has been determined by single crystal X-ray diffraction on $\{(BuSn)_{12}(\mu_3\text{-}O)_{14}(\mu_2\text{-}OH)_6\}(OH)_2(HOPr^i)_4$ and has revealed an equal amount of five- and six-coordinate tin atoms. As for its chloride analogues,[7,9] crystallization of this cluster relies on the formation of a framework of hydrogen bonds which involve the bridging hydroxo groups, the counterions, and the solvating molecules.

$(\{BuSn)_{12}O_{14}(OH)_6\}(OH)_2$ can be easily characterized in solution by ^{119}Sn NMR through its two resonances and their coupling satellites. Four J^2_{Sn-Sn} scalar coupling constants were observed and associated with different two bond paths between tin atoms in the molecular structure. The ^{1}H and ^{13}C NMR spectra are also quite characteristic of this cluster. Their complete assignment, performed with 1D and 2D NMR experiments, show that ^{1}H and ^{13}C NMR spectra also contain information about the coordination of tin and therefore can be useful tools for the characterization of this cluster in solution.

$\{(BuSn)_{12}(\mu_3\text{-}O)_{14}(\mu_2\text{-}OH)_6\}(OH)_2(HOPr^i)_4$ has also been characterized by the ^{119}Sn MAS NMR study. Its MAS spectrum is in good agreement with its solid state structure, even though the NMR result seems to indicate a higher symmetry for this compound. In the solid state, the hydrogen bond between the hydroxyl counterions and a specific hydroxy bridge is responsible for the higher number of tin environments observed by ^{119}Sn MAS NMR spectroscopy compared to ^{119}Sn solution NMR analysis. The shielding tensorial properties that have been extracted from the analysis of the spinning side bands bring new data for the correlation between structure and ^{119}Sn MAS NMR results. This cluster is also a nice reference for studies on related compounds that cannot be crystallized or dissolved, such as butylstannonic acid.

For hybrid organic−inorganic materials, the oxo−hydroxo butyltin cluster, $\{(BuSn)_{12}O_{14}(OH)_6\}(OH)_2$, can be considered as a stable and well-defined nanobuilding block. Transformation into a material is then a matter of establishing links between these clusters. For example, polymerizable organic groups, such as butenyl,[43] can be used instead of simple butyl chains. The so-obtained "functionalized clusters" can then be cross-linked by radical polymerization.[14] The cationic nature of this cluster can also be used to link them. For example, exchanging the hydroxyl counterions by dicarboxylates allows the construction of chains.[39] These approaches could provide very homogeneous coatings or membranes, with a high inorganic content.

Acknowledgment. We gratefully acknowledge Dr. D. Massiot (CRPHT-Orléans) for providing us a version of WINFIT, including the Herzfeld and Berger analysis of the tensorial properties.

Supporting Information Available: Tables of atomic coordinates, calculated atomic coordinates of hydrogen atoms and isotropic thermal parameters, anisotropic thermal parameters (U_{ij}) for non-hydrogen atoms, and bond lengths and angles and a packing diagram of the unit cell (21 pages). Ordering information is given on any current masthead page.

IC950144S

(43) Jousseaume, B.; Lahcini, M.; Rascle, M.-P.; Ribot, F.; Sanchez, C. *Organometallics* **1995**, *14*, 685.